Lévy walks and propagators in intermittent chaotic systems

G. Zumofen
Laboratorium für Physikalische Chemie, ETH-Zentrum, CH-8092 Zürich, Switzerland

J. Klafter
School of Chemistry, Tel-Aviv University, Tel-Aviv, 69978 Israel

A. Blumen
Theoretical Polymer Physics, University of Freiburg, W-7800 Freiburg, Germany
(Received 21 May 1992)

We study the propagator $P(r,t)$ for enhanced diffusion in intermittent chaotic systems represented by a class of iterated maps. The analysis is based on the velocity model, which is characterized by motion at a constant velocity with interruptions where sojourn times are chosen randomly but according to power-law distributions. The velocity model reproduces excellently the map-generated motion. The relationship to Lévy walks and scaling properties is discussed.

PACS number(s): 05.40.+j, 05.45.+b, 66.30.−h, 02.50.−r

Enhanced diffusion has been recently realized to be quite widespread and not just a peculiar example for deviations from Brownian motion [1–17]. Considerable interest has been attracted by this type of diffusion, which exhibits mean-square displacements that grow faster than linearly with time, $\langle r^2(t)\rangle \sim t^\alpha$, $\alpha>1$. In various model systems, enhanced diffusion has been observed for dynamics characterized by regular laminar motion interrupted by intermittent bursts [1,12–15]. It has been suggested that such anomalous behavior can be related to random walks in continuous time [1,15].

Enhanced diffusion shows up naturally in random-walk frameworks, such as Lévy walks, which were introduced in the context of dynamical systems and turbulent diffusion [2,4–9]. Lévy walks are based on space-time coupled memories and scale invariance of the motion events. For particular cases, the propagator is related to Lévy stable distributions. Lévy walks have been mainly studied within the jump model, where particles move instantaneously between sites after waiting some time at a site. Less studied has been the case where particles move continuously with a constant velocity between points of halt [7]. We call the latter case the velocity model [17].

In this Brief Report we analyze enhanced diffusion generated by iterated maps and show its one-to-one correspondence to the velocity model. We derive asymptotic expressions for the propagator and compare these results with those obtained from numerical calculations; excellent agreement is achieved.

For the dynamical system we use the concept of circle maps [1,15]:

$$x_{n+1}=g(x_n) , \tag{1}$$

where $g(x)$ denotes a map and n the number of iterations. The map is assumed to show reflection and translational symmetries:

$$g(-x)=-g(x) , \quad g(x+N)=g(x)+N . \tag{2}$$

Here N is an integer and denotes the unit cell of the particle position. With the rules of Eqs. (2) one has to define the map only in a reduced range, and we consider the map introduced by Geisel, Nierwetberg, and Zacherl [1]:

$$g(x)=(1+\epsilon)x+ax^z-1 , \quad 0\le x\le \tfrac{1}{2} . \tag{3}$$

This map is discontinuous at the cell boundaries. However, in order to preserve continuity within the cell we set $a=2^z(1-\epsilon/2)$ in Eq. (3). The quantity ϵ is a parameter which controls the numerical procedure in order to prevent the iteration from staying in a laminar phase beyond the typical time of observation. Now we determine the displacement $r(t)$ associated with a number t of iterations from

$$r(t)=x_{n+t}-x_n , \tag{4}$$

with x_0 chosen arbitrarily.

The map, Eq. (3), is characterized by a tangent contact $x_{n+1}\simeq x_n\pm 1$ for coordinates close to the cell boundaries: $|x-N|\to 0$. This gives rise to an almost laminar motion during long-time intervals (whose lengths depend on the injection coordinate into the laminar phase and on z). The laminar phases are followed by intermittent bursts typified by frequent changes of direction. This is demonstrated in Fig. 1, where a realization of $r(t)$ is plotted for 1000 iteration steps and for $z=\frac{5}{3}$. The inset shows the same characteristic behavior of the walk as the original figure, i.e., long and short steps occur on all scales, a fact exemplifying the self-affine properties of the walk.

For the probability of staying in a laminar phase, Geisel, Nierwetberg, and Zacherl [1] calculated the following probability distribution:

$$\psi(t)=\frac{2(2^{z-1}\epsilon-a)e^{\epsilon(z-1)t}}{[(2^{z-1}+a/\epsilon)^{\epsilon(z-1)t}-a/\epsilon]^{z/(z-1)}} \sim t^{-z/(z-1)} , \tag{5}$$

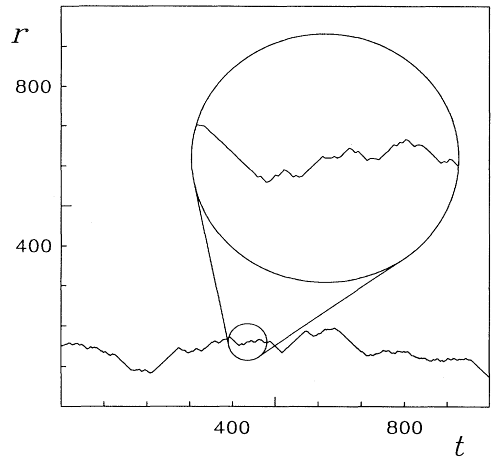

FIG. 1. The random walk obtained from 1000 steps of the iterated map, Eq. (4), for $z=\frac{5}{3}$ ($\mu=2.5$). The inset shows a part of the walk on an enlarged scale.

where the right-hand side of (5) holds for $1 \ll t \ll \epsilon^{-1}$. Making use of Eq. (5) and of renewal theory, Geisel, Nierwetberg, and Zacherl [1] derived a velocity-velocity correlation function from which they obtained the asymptotic form of the mean-square displacement $\langle r^2(t)\rangle$. Depending on z, three regimes were found: ballistic type, intermediate enhanced, and regular diffusion.

Here we concentrate on the whole distribution function, the propagator $P(r,t)$, which we calculate from the iterated map as follows:

$$P(r,t)=\langle \delta(r-x_{n+t}+x_n)\rangle , \tag{6}$$

where the average is taken over a set of initial iterations steps $\{n\}$. Usually, in the continuous-time random-walk (CTRW) framework, it is assumed that the first step has the same waiting-time distribution as all consecutive steps. To mimic this situation for the iterated maps, we require that the iterations of the set $\{n\}$ have to be injection steps into the laminar phase such that the first iteration samples the same typical waiting time distribution as all consecutive injection steps do. To achieve this requirement numerically, we assume that the iteration steps of the set $\{n\}$ have to take place during the intermittent burst and introduce the criterion $|x_{n+1}-x_n|<\frac{1}{2}$. To check the effectiveness of this criterion, we calculated $\psi(t)$, the probability distribution to stay in the laminar phase, and compared the asymptotic behavior with that of Eq. (5). If the average is taken over all iterations, the length distribution of the initial laminar phase of a sequence of iterations would differ from that of the following laminar phases and the process would correspond to the stationary-state situation encountered in CTRW approaches [18]; here we concentrate on the case of the nonstationary state.

Our analysis of the propagator is based on the space-time memory function $\psi(r,t)$, the probability distribution to move a distance r in time t in a single motion event. Usually, in CTRW analyses the motion is considered to occur by means of jumps between sites where the particle waits until the next jump takes place. In the velocity model, the particle is assumed to move at a constant velocity to a new location, where it chooses a new direction at random.

In the analytical description, this requirement is realized by means of the space-time-coupled memory function $\psi(r,t)=\frac{1}{2}\delta(|r|-t)\psi(t)$, where the δ function accounts for the constant velocity at which the particle moves between points of halt and $\psi(t)$ is given by Eq. (5). For simplicity, we consider dimensionless space and time variables. It is straightforward to show that an equivalent description of $\psi(r,t)$ is possible by writing $\psi(r,t)=\delta(|r|-t)\psi(r)$, where $\psi(r)$ denotes the distance distribution of a motion event. We adopt the latter description for our further derivations and have

$$\psi(r,t)\sim\delta(|r|-t)/|r|^{\mu} . \tag{7}$$

Comparing Eqs. (5) and (7), we may relate the two exponents μ and z to each other: $\mu\equiv z/(z-1)$.

A closed-form expression is obtained for the propagator in the Fourier-Laplace (k,u) space:

$$P(k,u)=\Psi(k,u)/[1-\psi(k,u)] . \tag{8}$$

Here, $\Psi(r,t)$ denotes the probability to *pass* at position r at time t in a single motion sojourn and is given by a cumulative type of distribution:

$$\Psi(r,t)\sim\delta(|r|-t)\sum_{j\geq|r|} j^{-\mu} . \tag{9}$$

For the Fourier-Laplace transformation of $\psi(r,t)$ needed in Eq. (8), we choose the representation

$$\psi(k,u)=\tfrac{1}{2}[\phi(q)+\phi(\bar{q})] , \tag{10}$$

with $q=u+ik$ and $\bar{q}=u-ik$ and with

$$\phi(q)=A\sum_{r>0} e^{-qr}r^{-\mu} . \tag{11}$$

Following the derivation in Ref. [8], we obtain for small q

$$\phi(q)\simeq\begin{cases}1+c_\mu q^{\mu-1} , & 1<\mu<2\\ 1-c_1q+c_\mu q^{\mu-1} , & 2<\mu<3\\ 1-c_1q+c_2q^2+c_\mu q^{\mu-1} , & 3<\mu<4 .\end{cases} \tag{12}$$

For integer subscripts, the constants are $c_j=\zeta(\mu-j)/[j!\zeta(\mu)]$, while $c_\mu=\Gamma(1-\mu)/\zeta(\mu)$. Approximating the sum in Eq. (9) by an integral, we derive

$$\Psi(k,u)\simeq\frac{1}{2q}[1-\phi(q)]+\frac{1}{2\bar{q}}[1-\phi(\bar{q})] . \tag{13}$$

According to the findings for the mean-squared displacement, we distinguish among three characteristic regimes: ballistic type, intermediate enhanced, and regular diffusion. These regimes are characterized by the three μ ranges in Eq. (12) and by the corresponding z values. For the asymptotic long-time behavior of the propagator, we obtain the following scaling representation:

$$P(r,t)=f(\xi)/\tau \; , \tag{14}$$

where ξ is the scaling variable, $\xi=|r|/\tau$, and where

$$\tau=\begin{cases} t \; , & 1<\mu<2 \\ t^{1/(\mu-1)} \; , & 2<\mu<3 \\ t^{1/2} \; , & 3<\mu \; . \end{cases} \tag{15}$$

$f(\xi)$ in Eq. (14) denotes the scaling function, which we studied analytically and numerically. Here we present only the main results. For the ballistic-type regime, $1<\mu<2$, $f(\xi)$ is constant for small ξ and diverges when ξ approaches the value 1. This becomes obvious for the particular case of $\mu=\frac{3}{2}$, for which we obtained the asymptotic expression

$$f(\xi)=\pi^{-1}(1-\xi^2)^{-1/2} \; , \quad \xi\le 1 \; , \quad \mu=\tfrac{3}{2} \; . \tag{16}$$

It is in this regime where the results presented here deviate qualitatively from those obtained for the jump model with space-time-coupled memories [8].

For the intermediate enhanced and regular regimes, $2<\mu<4$, we observe a Gaussian behavior for small ξ followed by a power-law wing:

$$f(\xi)\sim\begin{cases} \exp(-c\xi^2) \; , & \xi<1 \\ \xi^{-\mu} \; , & 1<\xi \text{ and } r<t \\ 0 \; , & r>t \; . \end{cases} \tag{17}$$

For $\mu>3$, scaling is not obeyed for $\xi>1$, but the decay follows the same poer law, namely $P(r,t)\sim t/r^{\mu}$. For small-μ values, $P(r,t)$ tends to diverge for $r\to t$. In the intermediate regime, $2<\mu<3$, the expression of $P(r,t)$ is similar to Lévy-stable distributions.

In Figs. 2–4 we compare the propagators obtained directly from the iterated maps, Eq. (6), with those obtained from a numerical calculation of $P(r,t)$, Eq. (8), and with the asymptotic scaling forms, Eqs. (15)–(17). For the maps 10^{10} iterations were performed. The parameter ϵ was set to 10^{-6} for $\mu=1.5$ and was set to zero for $\mu=2.5$ and 3.5. In Fig. 2 the map results are compared with the analytic form, Eq. (16). In Figs. 3 and 4 the decay in the wings is compared with the theoretical slope $\xi^{-\mu}$. The data collapse for various times indicates that scaling is obeyed.

The propagator of the velocity model was calculated from a numerical Fourier-Laplace transform of Eqs. (7) and (9) followed by a numerical Fourier-Laplace inver-

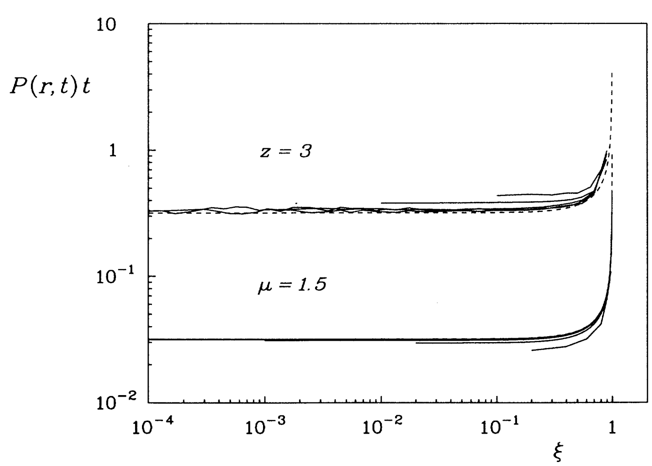

FIG. 2. The propagator in the ballistic-type regime, plotted as $tP(r,t)$. The upper curves are the results of the iterated map, Eq. (6), for $z=3$ and for times $t=10$, 10^2, 10^3, 10^4, and 10^5. The lower curves indicate the numerical results of the propagator, Eq. (8), for $\mu=1.5$ and for the same sequence of times, shifted vertically by an order of magnitude. The broken lines give the analytical asymptotic form, Eq. (16). The scaling variable is $\xi=r/t$.

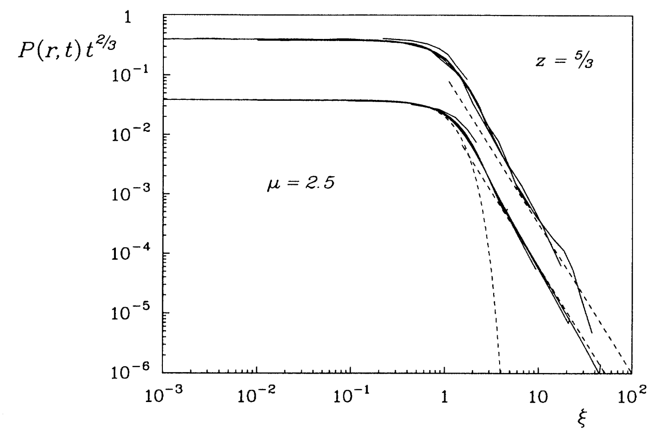

FIG. 3. Same as in Fig. 2, here plotted is $t^{2/3}P(r,t)$ for $z=\frac{5}{3}$ (upper curves), where the theoretical slope for large ξ is indicated by a dashed line, and for $\mu=2.5$ (lower curves), where the dashed lines give the analytical asymptotic forms, Eq. (17). The scaling variable is $\xi=r/t^{2/3}$ and the regime is that of enhanced diffusion.

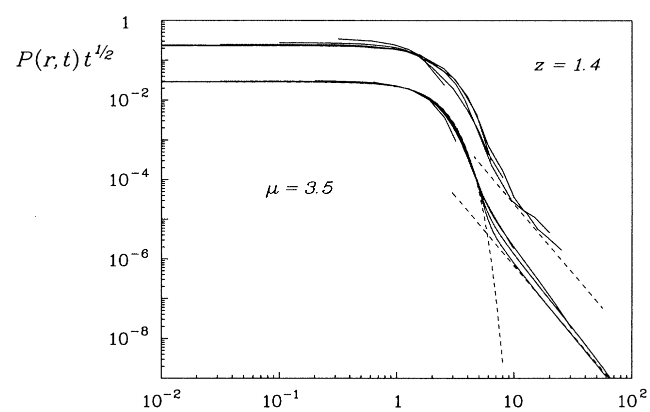

FIG. 4. Same as in Fig. 2, here $t^{1/2}P(r,t)$ is plotted for $z=1.4$ (upper curves), where the theoretical slope for large ξ is indicated by a dashed line and for $\mu=3.5$ (lower curves), where the dashed lines give the Gaussian behavior for $\xi<1$, Eq. (16) and the power law $t/[2\zeta(\mu-1)r^{\mu}]$, $t=10^5$ for $\xi>1$, respectively. The scaling variable is $\xi=r/t^{1/2}$ and the regime is that of regular diffusion.

sion of Eq. (8). For short times, $t \leq 100$, an exact enumeration procedure was applied. Scaling is observed in all cases except in the wing for $\mu=3.5$. The results are presented in Figs. 2–4 and are close to those obtained for the jump model in Ref. [8] except for the ballistic-type case, $\mu=1.5$, where the results of the two models deviate qualitatively.

In summary, we have studied the propagators obtained from iterated maps in the enhanced-diffusion regime. We have introduced the CTRW velocity model, which provides an analytical description of the enhanced-diffusion process, and we have shown that this model offers an effective probabilistic means to describe anomalous diffusion in deterministic systems.

We thank Professor K. Dressler, Dr. R. Stoop, and G. Poupart for helpful discussions, and F. Weber for technical assistance. J.K. thanks the ETH for the hospitality during the time this work was carried out. A grant of computer time from the Rechenzentrum der ETH-Zürich and the support of the Deutsche Forschungsgemeinschaft (SFB 60) and of the Fonds der Chemischen Industrie are gratefully acknowledged.

[1] T. Geisel, J. Nierwetberg, and A. Zacherl, Phys. Rev. Lett. **54**, 616 (1985).
[2] M. F. Shlesinger and J. Klafter, Phys. Rev. Lett. **54**, 2551 (1985).
[3] J.-P. Bouchaud and A. Georges, Phys. Rep. **195**, 127 (1990).
[4] J. Klafter, A. Blumen, and M. F. Shlesinger, Phys. Rev. A **35**, 3081 (1987).
[5] M. F. Shlesinger and J. Klafter, in *Transport and Relaxation in Random Materials,* edited by J. Klafter, R. J. Rubin, and M. F. Shlesinger (World Scientific, Singapore, 1986).
[6] M. F. Shlesinger, B. West, and J. Klafter, Phys. Rev. Lett. **58**, 1100 (1987).
[7] M. F. Schlesinger and J. Klafter, J. Phys. Chem. **93**, 7023 (1989).
[8] G. Zumofen, J. Klafter, and A. Blumen, Chem. Phys. **146**, 433 (1990).
[9] G. Zumofen, J. Klafter, and A. Blumen, J. Stat. Phys. **65**, 991 (1991).
[10] J. Masoliver, K. Lindenberg, and G. H. Weiss, Physica A **157**, 891 (1989).
[11] M. Araujo, S. Havlin, G. H. Weiss, and H. E. Stanley, Phys. Rev. A **43**, 5207 (1991).
[12] A. S. Pikovsky, Phys. Rev. A **43**, 3146 (1991).
[13] I. S. Aranson, M. I. Rabinovich, and L. Sh. Tsimring, Phys. Lett. A **151**, 523 (1990).
[14] X.-J. Wang, Phys. Rev. A **41**, 8407 (1992); R. N. Mantegna, J. Stat. Phys. (to be published).
[15] P. Manneville, J. Phys. (Paris) **41**, 1235 (1980).
[16] G. M. Zaslavasky and M. K. Tippett, Phys. Rev. Lett. **67**, 3251 (1991).
[17] G. Zumofen, J. Klafter, and A. Blumen (unpublished).
[18] W. Feller, *An Introduction in Probability Theory and Applications,* 2nd ed. (Wiley, New York, 1971), Vol. 2.